Journal of Medicinal Chemistry

ARTICLE

pubs.acs.org/jmc

Optimization of Cellular Activity of G9a Inhibitors 7-Aminoalkoxy-quinazolines

Feng Liu,[†,∥] Dalia Barsyte-Lovejoy,[‡,∥] Abdellah Allali-Hassani,[‡] Yunlong He,[§] J. Martin Herold,[†] Xin Chen,[†] Christopher M. Yates,[⊥] Stephen V. Frye,[†] Peter J. Brown,[‡] Jing Huang,[§] Masoud Vedadi,[‡] Cheryl H. Arrowsmith,[‡] and Jian Jin*[,†]

[†]Center for Integrative Chemical Biology and Drug Discovery, Division of Medicinal Chemistry and Natural Products, UNC Eshelman School of Pharmacy, University of North Carolina at Chapel Hill, Chapel Hill, North Carolina 27599, United States

[‡]Structural Genomics Consortium, University of Toronto, Toronto, Ontario, M5G 1L7, Ontario, Canada

[§]Laboratory of Cancer Biology and Genetics, National Cancer Institute, National Institutes of Health, Bethesda, Maryland 20892, United States

Supporting Information

ABSTRACT: Protein lysine methyltransferase G9a plays key roles in the transcriptional repression of a variety of genes via dimethylation of lysine 9 on histone H3 (H3K9me2) of chromatin as well as dimethylation of nonhistone proteins including tumor suppressor p53. We previously reported the discovery of UNC0321 (**3**), the most potent G9a inhibitor to date, via structure-based design and structure−activity relationship (SAR) exploration of the quinazoline scaffold represented by BIX01294 (**1**). Despite its very high in vitro potency, compound **3** lacks sufficient cellular potency. The design and synthesis of several generations of new analogues aimed at improving cell membrane permeability while maintaining high in vitro potency resulted in the discovery of a number of novel G9a inhibitors such as UNC0646 (**6**) and UNC0631 (**7**) with excellent potency in a variety of cell lines and excellent separation of functional potency versus cell toxicity. The design, synthesis, and cellular SAR of these potent G9a inhibitors are described.

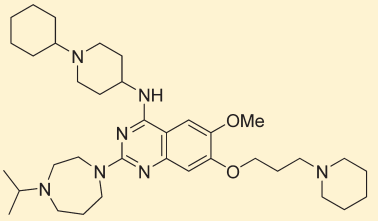

G9a IC_{50} = 6 nM
Reduction of H3K9me2 in MCF7 cells: IC_{50} = 10 nM
Cell toxicity (MCF7 cells): EC_{50} = 4,700 nM

INTRODUCTION

The "writers" (the enzymes that produce post-translational modifications (PTMs)), the "readers" (the proteins that recognize PTMs), and the "erasers" (the enzymes that remove PTMs) of the histone code[1,2] are critical targets for manipulation to understand the role of the histone code in human disease. Protein lysine methyltransferases (PKMTs), the methyl "writers" of the histone code, catalyze the transfer of a methyl group from *S*-adenosyl-L-methionine (SAM) to the ε-amino group of lysine residues of various proteins including histones and nonhistone proteins.[3,4] With the exception of DOT1L, all PKMTs contain the evolutionarily conserved SET domain, named after *Drosophila* Su(var.)3−9 (suppressor of variegation 3−9), E(z) (enhancer of zeste), and trithorax.[5] Since the first PKMT was characterized in 2000,[6] more than 50 human PKMTs have been identified[3,4] and the mechanistic, biochemical, and biological functions of these proteins are still being elucidated. PKMTs display significant variations in protein substrate selectivity and the degree of methylation on lysine from mono- and di-, to trimethylation. In the context of epigenetic gene regulation, these different states of lysine methylation encode distinct signals and are recognized by a host of protein modules such as Tudor and chromodomains, MBT domains and PHD fingers, usually within larger proteins, and chromatin remodeling complexes that direct cellular processes such as chromatin packaging and transcriptional regulation, and DNA repair, replication and metabolism.[7,8] PKMTs themselves are also often components of large regulatory complexes and act in concert with other epigenetic factors.[9] Selective inhibition of individual PKMT catalytic activity in cellular systems represents a valuable strategy to decipher the complex signaling mechanisms of histone and protein lysine methylation. A "toolkit" of potent, selective, and cell-penetrant chemical probes[10] of PKMTs will permit biological and therapeutic hypotheses to be tested with high confidence in cell-based models of human biology and disease. However, very few such small-molecule tools are available to the biomedical research community.[11−13]

G9a (also known as KMT1C or EHMT2) was initially identified as a H3K9 methyltransferase.[14] It was later found that G9a could methylate various histone[15] and nonhistone proteins including the tumor suppressor p53.[16,17] G9a is overexpressed in various human cancers,[17−20] and knockdown of G9a inhibits cancer cell growth.[18,20−22] The dimethylation of p53 K373 by G9a and GLP (also known as KMT1D or EHMT1), a closely related methyltransferase that shares 80% sequence identity with G9a in their respective SET domains and forms a heterodimer with G9a, results in the inactivation of p53, whose loss of function is implicated in over 50% of cancers.[17] In addition, G9a has been

Received: July 10, 2011
Published: July 22, 2011

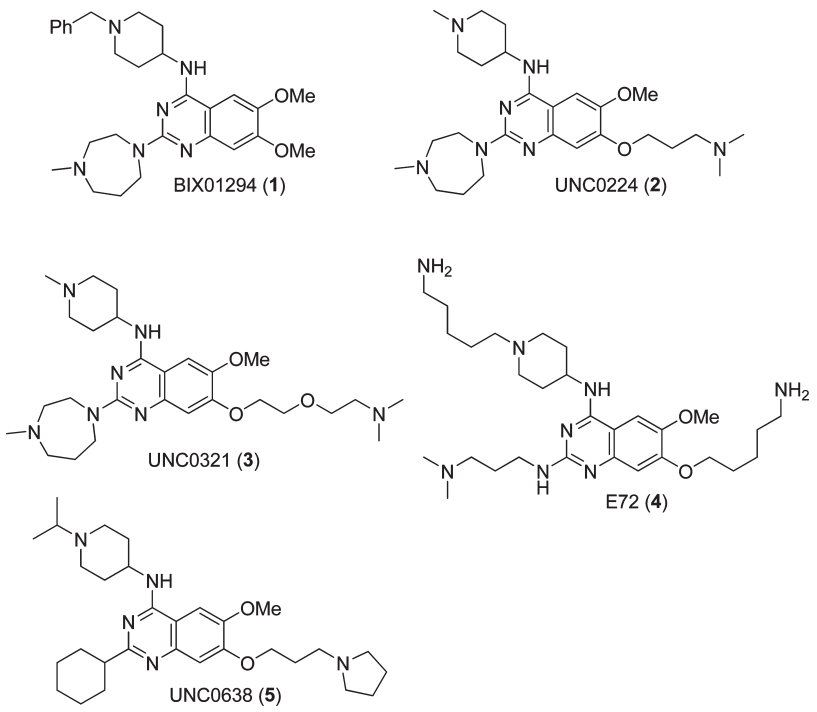

Figure 1. Structures of known G9a/GLP inhibitors.[29,31−34]

shown to play a role in cocaine addiction,[23] mental retardation,[24] maintenance of HIV-1 latency,[25] and DNA methylation in embryonic stem (ES) cells.[26−28]

The recent report by Jenuwein and colleagues of BIX01294 (**1**), the first selective small molecule inhibitor of G9a and GLP,[29,30] was an important advance in the PKMT probe discovery area (Figure 1). We have explored the 2,4-diamino-6,7-dimethoxyquinazoline template represented by **1**. Our initial structure-based design and synthesis in combination with SAR exploration led to the discovery of potent and selective G9a inhibitors UNC0224 (**2**) and UNC0321 (**3**, the most potent G9a inhibitor (Morrison K_i = 63 pM) to date) and valuable SAR for the quinazoline template.[31,32] Cheng and co-workers have also reported SAR of the quinazoline scaffold that resulted in the discovery of E72 (**4**) as a potent and selective GLP inhibitor.[33] However, compounds **3**[34] and **4**[33] are less potent in cellular assays than **1** even though **3** and **4** are more potent than **1** in in vitro biochemical assays. Compound **1** is active at reducing the H3K9me2 levels in bulk histones and at G9a target genes,[29] but it has poor separation of functional potency versus cell toxicity.[29,34] We have recently reported UNC0638 (**5**), a chemical probe of G9a/GLP with robust on-target activities in cells and an excellent ratio of toxicity to functional potency (tox/function ratio, which is determined dividing the EC_{50} value of the observed toxicity by the IC_{50} value of the functional potency).[34] Here we report the design and synthesis of novel analogues of compound **3** aimed at improving cellular potency of this quinazoline series and the SAR of these compounds in cell-based assays that led to the discovery of compound **5** and novel G9a inhibitors such as UNC0646 (**6**) and UNC0631 (**7**), which have excellent tox/function ratios in a variety of cell lines.

RESULTS AND DISCUSSION

It was hypothesized that the poor cellular potency of compound **3** was likely due to its poor cell membrane permeability and low lipophilicity (ALogP = 1.9). To improve cell membrane permeability, and thus cellular potency of this chemical series, we exploited the SAR at the 2-amino, 4-amino, and 7-aminoalkoxy regions of this quinazoline scaffold discovered previously. For the 7-aminoalkoxy region, the four groups (marked in blue in Figure 2) that yield high in vitro potency[32] were selected as affinity anchors. Because few modifications to the 4-(piperidin-4-yl)amino moiety

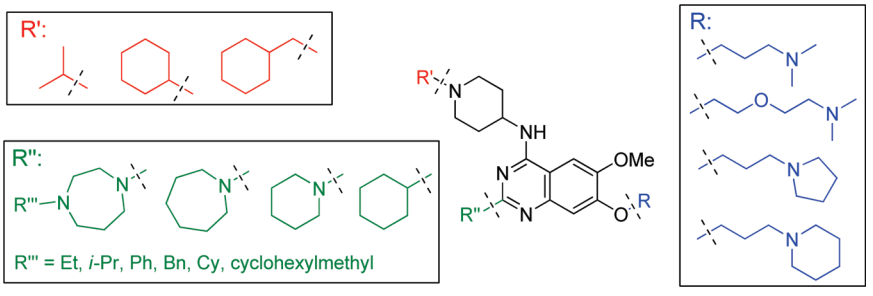

Figure 2. Compounds designed to achieve balanced in vitro potency and physicochemical properties aiding cell penetration to improve cellular potency.

dx.doi.org/10.1021/jm200903z |J. Med. Chem. 2011, 54, 6139–6150

Table 1. SAR of the 7-Aminoalkoxy Region[a]

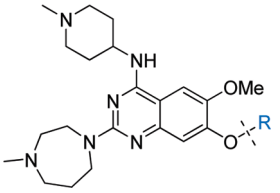

Compound ID	R	G9a IC_{50} (μM) (SAHH-coupled Assay)	Cellular IC_{50} (μM) (Reduction of H3K9me2 (ICW))	Cell Toxicity EC_{50} (μM) (MTT)	ALogP[b]
2	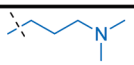	0.043	> 5.0	34	2.1
3	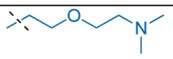	0.009	11	> 40	1.9
8	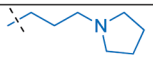	0.008	2.2	15	2.6
9	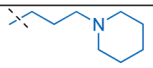	0.025	0.91	12	3.0

[a] IC_{50} or EC_{50} values are the average of at least duplicate assay runs with standard deviation (SD) values that are 3-fold less than the average. [b] ALogP values were calculated using Pipeline Pilot v7.5.

Scheme 1. Synthesis of Compounds 17[a]

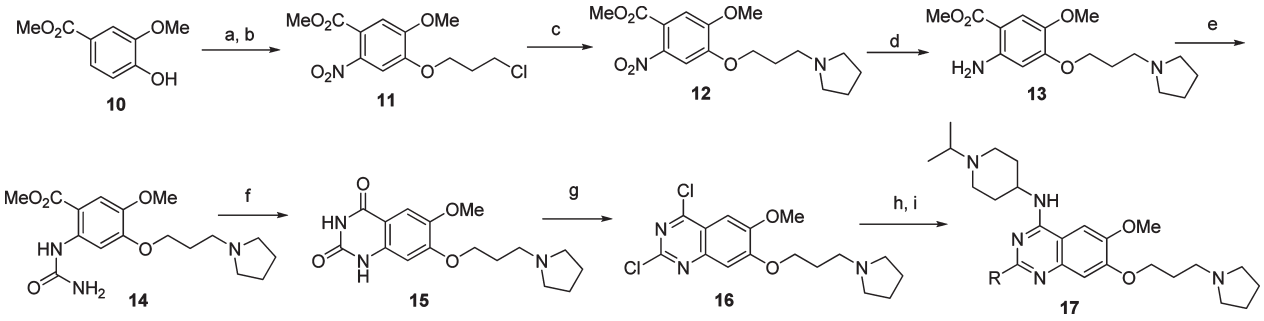

[a] (a) 1-Chloro-3-iodopropane, K_2CO_3, CH_3CN, reflux; (b) HNO_3, Ac_2O, 0 °C to rt, 75% over two steps; (c) pyrrolidine, K_2CO_3, NaI, cat. tetrabutylammonium iodide, CH_3CN, reflux, 81%; (d) Fe dust, NH_4OAc, AcOEt−H_2O, reflux, 63%; (e) NaOCN, AcOH, H_2O, rt; (f) NaOH, H_2O, MeOH, reflux; (g) *N*,*N*-diethylaniline, $POCl_3$, reflux, 50% over three steps; (h) 1-isopropylpiperidin-4-amine, DIEA, THF, rt, 94%; (i) various amines, CF_3COOH, *i*-PrOH, 160 °C, microwave, 74−82%.

except the *N*-capping group (which does not make interactions with the protein) on the piperidine nitrogen are tolerated,[31,32] the three *N*-capping groups (marked in red in Figure 2) were selected to increase lipophilicity while maintaining high in vitro potency. Because modifications to the 2-amino moiety are well tolerated,[31,32] various homopiperazine, azepine, piperidine, and cyclohexyl groups (marked in green in Figure 2) were selected to further increase lipophilicity. These combination compounds were designed to achieve balanced in vitro potency and physicochemical properties aiding cell penetration.

The inhibitory activity of these compounds on G9a was evaluated using the fluorescence-based *S*-adenosyl-L-homocysteine hydrolase (SAHH)-coupled assay[32] that we previously reported. The H3K9me2 antibody cell immunofluorescence In-Cell Western (ICW) assay,[34] recently developed by us, was used to assess the cellular potency of these compounds. This assay allows rapid processing of multiple compounds for H3K9me2 immunofluorescence signal and normalization to cell number via the use of the nucleic acid dye DRAQ5. The compounds were first evaluated in MDA-MB-231 cells because this cell line possesses robust H3K9me2 levels. Most promising compounds were subsequently evaluated in a number of other cancer and normal cell lines. Viability of cells after inhibitor treatment was assessed by an MTT (3-(4,5-dimethylthiazol-2-yl)->2,5-diphenyl tetrazolium bromide) assay, which measures the conversion of yellow MTT to purple formazan by cellular mitochondrial reductase.

For the 7-aminoalkoxy region, compounds **2**, **3**, **8**, and **9**, the four most potent G9a inhibitors (in biochemical assays) that we

dx.doi.org/10.1021/jm200903z |*J. Med. Chem.* 2011, 54, 6139–6150

Table 2. SAR of the 2-Amino Region[a]

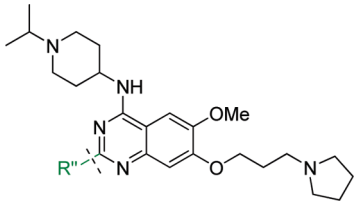

Compound ID	R''	G9a IC_{50} (μM) (SAHH-coupled Assay)	Cellular IC_{50} (μM) (Reduction of H3K9me2 (ICW))	Cell Toxicity EC_{50} (μM) (MTT)	Tox/function Ratio (MTT EC_{50}/ICW IC_{50})	ALogP[b]
17a	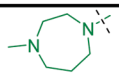	0.010	0.52	1.4	3	3.3
17b	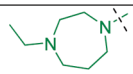	0.005	0.47	1.7	4	3.2
17c	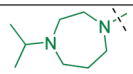	0.002	0.34	4.5	13	3.5
17d	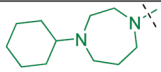	0.022	0.10	0.73	7	4.7
17e	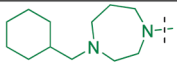	0.007	0.093	0.76	8	5.0
17f	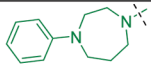	0.010	0.22	2.1	10	4.5
17g	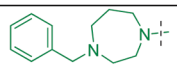	0.009	0.058	0.6	10	4.4
17h		0.016	0.15	7.0	47	3.7
17i		0.020	0.10	5.7	57	4.2
5		0.012	0.081	11	140	4.8

[a] IC_{50} or EC_{50} values are the average of at least duplicate assay runs with standard deviation (SD) values that are 3-fold less than the average. [b] ALogP values were calculated using Pipeline Pilot v7.5.

previously reported,[32] were evaluated in the ICW and MTT assays (Table 1). Similar to compound **3**, compound **2** showed poor potency in reducing H3K9me2 levels in MDA-MB-231 cells even though it was highly potent in the G9a enzyme inhibitory assay. On the other hand, compounds **8** and **9**, which are more lipophilic than compounds **2** and **3** as evident by their ALogP values, showed higher cellular potency in the ICW assay. All four compounds had low cell toxicity (EC_{50} > 10 μM) in the MTT assay. These initial findings validated our hypothesis that the poor cellular potency of compound **3** was due to its low lipophilicity, and high cellular potency could be achieved by increasing lipophilicity of this series. On the basis of these results, we selected the pyrrolidin-1-ylpropoxy (**8**) and piperidin-1-ylpropoxy (**9**) groups as the preferred 7-aminoalkoxy moieties for optimizing other regions of this quinazoline series.

To efficiently explore the 2-amino region, a new synthetic route (9 steps) was developed (Scheme 1). Unlike our previously published synthetic route,[32] this new synthesis allows us to install various 2-amino groups at the last step of the synthetic sequence. Commercially available methyl 4-hydroxy-3-methoxybenzoate (**10**) was reacted with 1-chloro-3-iodopropane, followed by nitration, to afford the chloride **11**. Substitution of the chloride with pyrrolidine and subsequent reduction of the nitro group yielded the aniline **13**. Formation of urea from the aniline **13** and subsequent ring closure afforded the intermediate **15**, which was then converted to the 2,4-dichloroquinazoline **16**. Two

dx.doi.org/10.1021/jm200903z |J. Med. Chem. 2011, 54, 6139–6150

consecutive chloro displacement reactions by various amines provided the desired final products **17a**−**17i** in good overall yields. Synthesis of compound **5**, the 2-cyclohexyl analogue of compounds **17a**−**17i**, from the intermediate **13** was reported by us previously.[34]

Compounds **17a**−**17i** and **5** were highly potent inhibitors (IC_{50} < 0.025 μM) in the G9a SAHH-coupled biochemical assay (Table 2). Various *N*-capping groups (**17a**−**17g**) on the outer nitrogen of the homopiperazine moiety were well tolerated. In addition, azepane (**17i**), piperidine (**5**), and cyclohexyl groups (**5**) also showed high in vitro potency. Importantly, in addition to maintaining high in vitro potency, these new compounds have improved lipophilicity compared to compounds **2** and **3**. We were pleased to find that the combination of high in vitro potency and improved lipophilicity indeed resulted in high cellular potency (IC_{50} < 0.5 μM in the ICW assay). In particular, more lipophilic compounds such as **17d** (ALogP 4.7), **17e** (ALogP 5.0), **17g** (ALogP 4.4), **17i** (ALogP 4.2), and **5** (ALogP 4.8) had cellular potency (IC_{50}) equal to or less than 0.1 μM. Plotting cellular potency of the inhibitors in Tables 1 and 2 and inhibitors to be discussed below as a function of ALogP values of these inhibitors reveals that cellular potency strongly correlates with lipophilicity (Figure 3). These results validated our design strategy for improving cellular potency. Furthermore, cell toxicity of these highly potent G9a inhibitors was assessed using the MTT assay. While most of these inhibitors had a relatively poor tox/function ratio (<10), compounds **17h**, **17i**, and **5** had a good separation of functional potency (reducing H3K9me2 levels) versus cell toxicity (tox/function ratio >45). In particular, compound **5** had an excellent tox/function ratio of 140.

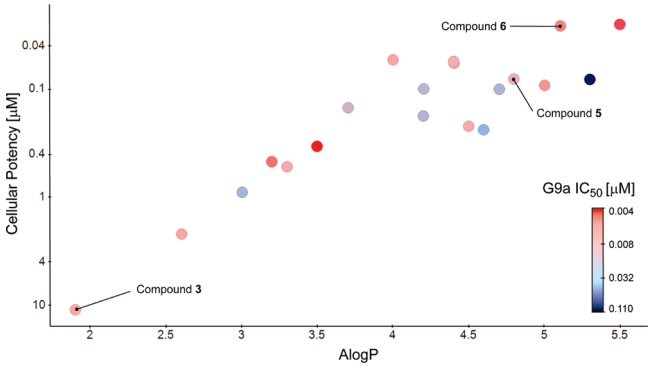

Figure 3. Analysis of cellular potency of G9a inhibitors as a function of their ALogP values reveals that cellular potency increases as lipophilicity increases for inhibitors that have similar in vitro potency. The inhibitors are color-coded with their G9a in vitro potency.

Because compound **5** showed high cellular potency and excellent separation of functional potency versus cell toxicity, we further investigated this 2-cyclohexyl quinazoline subseries. Thus, a new 9-step synthesis (Scheme 2) was developed to efficiently explore the 7-aminoalkoxy region. Benzyl protection of commercially available 4-hydroxy-3-methoxybenzonitrile (**18**), followed by nitration and subsequent reduction, afforded the aniline **19**. Amide formation from the aniline **19** and subsequent cyclization yielded the quinazolinone **20**, which was then converted to the 4-chloro quinazoline **21**. Displacement of the chloro intermediate **21** with 1-isopropylpiperidin-4-amine, followed by debenzylation, afforded the phenol **23**. Mitsunobu reactions of the phenol **23** with various amino alcohols yielded the desired compounds **24a**, **24b**, and **5**.

Compared to compound **5**, compound **24a** was less potent in the ICW assay (Table 3). This is likely due to the about 10-fold lower potency of compound **24a** in the G9a biochemical assay although **24a** is slightly more lipophilic. The combination of lower in vitro potency and lower lipophilicity of compound **24b** compared to compound **5** resulted in lower cellular potency as expected (Figure 3). Interestingly, both compounds **24a** and **24b** had low cell toxicity, similar to compound **5**.

We next synthesized a number of combination compounds including **6**, **7**, and **25** − **27** using the synthetic route outlined in Scheme 1 and evaluated them in the G9a SAHH-coupled, ICW, and MTT assays. Compounds **6**, **7**, **25**, and **26**, which had high in vitro potency versus G9a and improved lipophilicity, were highly potent (IC_{50} < 0.06 μM) in reducing H3K9me2 levels in MDA-MB-231 cells and had low cell toxicity (Table 4). In particular, compounds **6** and **7** were more potent than compound **5** and had a similar tox/function ratio in MDA-MB-231 cells (Table 5). On the other hand, many combination compounds failed to improve cellular potency and reduce cell toxicity. For example, compound **27** was about 10-fold less potent in reducing cellular levels of H3K9me2 than compounds **6** and **7**. The lower cellular potency of compound **27** is

Scheme 2. Synthesis of Compounds 24 and 5[a]

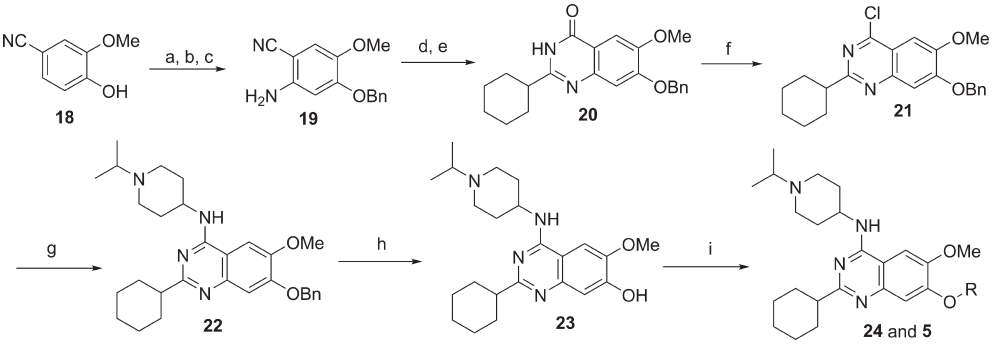

[a] (a) BnBr, K_2CO_3, DMF, rt; (b) HNO_3, Ac_2O, 0 °C to rt; (c) Fe dust, NH_4Cl, *i*-PrOH-H_2O, reflux, 67% over 3 steps; d) cyclohexane carbonyl chloride, DIEA, DMF-DCM, 0 °C to rt; (e) NaOH, H_2O_2, EtOH, reflux, 48% over 2 steps; (f) *N*,*N*-diethylaniline, $POCl_3$, reflux, 79%; (g) 1-isopropylpiperidin-4-amine, DIEA, *i*-PrOH, 160 °C, microwave, 94%; (h) Pd/C, 1,4-cyclohexadiene, EtOH, reflux; (i) various amino alcohols, PPh_3, DIAD, THF, 0 °C to rt, 36−65% over 2 steps.

dx.doi.org/10.1021/jm200903z |*J. Med. Chem.* 2011, 54, 6139–6150

Table 3. SAR of 2-Cyclohexyl Quinazoline Analogues[a]

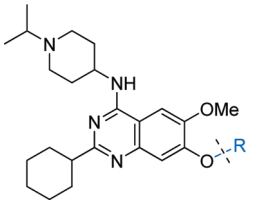

Compound ID	R	G9a IC_{50} (μM) (SAHH-coupled Assay)	Cellular IC_{50} (μM) (Reduction of H3K9me2 (ICW))	Cell Toxicity EC_{50} (μM) (MTT)	ALogP[b]
5	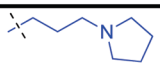	0.012	0.081	11	4.8
24a	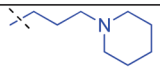	0.11	0.26	7.6	5.3
24b	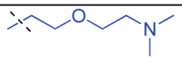	0.021	0.18	13	4.2

[a] IC_{50} or EC_{50} values are the average of at least duplicate assay runs with standard deviation (SD) values that are 3-fold less than the average. [b] ALogP values were calculated using Pipeline Pilot v7.5.

Table 4. Cellular Potency and Cell Toxicity of Combination Compounds[a]

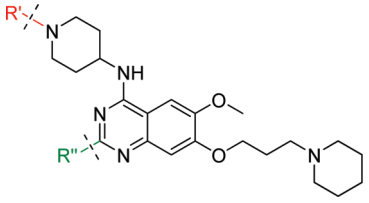

Compound ID	R''	R'	G9a IC_{50} (μM) (SAHH-coupled Assay)	Cellular IC_{50} (μM) (Reduction of H3K9me2 (ICW))	Cell Toxicity EC_{50} (μM) (MTT)	ALogP[b]
6 (UNC0646)	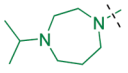		0.006	0.026	3.3	5.1
7 (UNC0631)			0.004	0.025	2.8	5.5
25			0.008	0.054	4.1	4.0
26	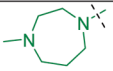		0.011	0.056	2.9	4.4
27			0.031	0.24	6.6	4.6

[a] IC_{50} or EC_{50} values are the average of at least duplicate assay runs with standard deviation (SD) values that are 3-fold less than the average. [b] ALogP values were calculated using Pipeline Pilot v7.5.

likely due to the combination of its lower G9a in vitro potency and lower lipophilicity compared to compounds **6** and **7** (Figure 3).

Because compounds **6** and **7** showed excellent separation of functional potency versus cell toxicity in MDA-MB-231 cells, these

dx.doi.org/10.1021/jm200903z |J. Med. Chem. 2011, 54, 6139–6150

Table 5. Potency and Toxicity of Compounds 5, 6, and 7 in a Variety of Cell Lines[a]

		ICW IC_{50} (μM)			MTT EC_{50} (μM)			tox/function ratio (MTT EC_{50}/ICW IC_{50})		
		5	6	7	5	6	7	5	6	7
breast carcinoma	MDA-MB-231	0.081	0.026	0.025	11	3.3	2.8	140	130	110
	MCF7	0.070	0.010	0.018	7.6	4.7	1.7	110	470	94
prostate carcinoma	PC3	0.059	0.012	0.026	14	2.8	3.8	240	230	150
	22RV1	0.048	0.014	0.024	4.5	7.2	2.5	94	510	100
colon carcinoma	HCT116 wt	0.21	0.068	0.051	11	8.7	5.8	52	130	110
	HCT116 p53−/−	0.24	0.086	0.072	11	12	6.4	46	140	89
human fibroblast	IMR90	0.12	0.010	0.046	2.3	3.6	1.8	19	360	39

[a] IC_{50} or EC_{50} values are the average of at least duplicate assay runs with standard deviation (SD) values that are 3-fold less than the average.

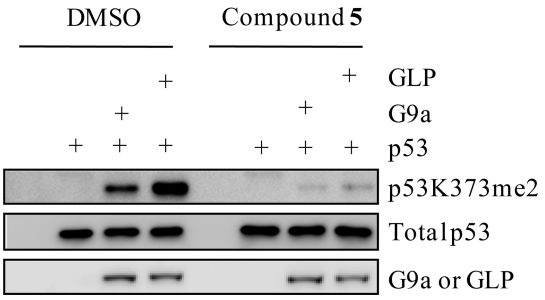

Figure 4. Compound **5** at 0.25 μM effectively inhibited the dimethylation of p53 K373 in H1299 cells. p53 expression vector was cotransfected with or without expression vectors for G9a or GLP into H1299 cells. Immediately after transfection, cells were treated with compound **5** or DMSO for 24 h. Cellular levels of p53 K373me2, total p53 and G9a or GLP were subject to Western blot analysis using antibodies.

two compounds were further evaluated in a variety of cell lines to characterize their cellular potency and cell toxicity. As shown in Table 5, compounds **6** and **7** were highly potent in reducing H3K9me2 levels in these cell lines and had low cell toxicity. Similar to compound **5**, compounds **6** and **7** had excellent tox/function ratios in these cell lines. In particular, compound **6** had an outstanding tox/function ratio in MCF7 (470), 22RV1 (510), and IMR90 (360) cells, making this compound potentially more useful for investigating G9a biology in these specific cell lines. In general, compounds **6** and **7** had higher cellular potency but also higher cell toxicity compared to compound **5**. While compound **5** has been selected as a chemical probe of G9a/GLP[34] because of its low cell toxicity and lower molecular weight, compounds **6** and **7** are valuable alternative tool compounds that may be more suitable for investigating specific cellular systems (vide supra).

The excellent selectivity of compound **5** for G9a/GLP over a wide range of epigenetic and nonepigenetic targets has been reported previously.[34] Consistent with these results, we found that compound **6** was also a potent GLP inhibitor (IC_{50} < 0.015 μM in the GLP SAHH-coupled assay) and highly selective for G9a/GLP over several other PKMTs and PRMTs including SETD7 (a H3K4 PKMT), SUV39H2 (a H3K9 PKMT), SETD8 (a H4K20 PKMT), and PRMT3 (IC_{50} > 10 μM in the SAHH-coupled assays against these four targets).

In addition to methylating histone substrates,[14,15,35] G9a and GLP dimethylate K373 of the tumor suppressor p53.[17] We reported the robust effects of compound **5** on reducing H3K9me2 levels in various cellular systems.[34] However, the effects of the quinazoline series on cellular levels of p53 K373me2 have not been reported previously. Thus, we evaluated the effects of compound **5** on reducing p53 K373me2 levels in H1299 cells (p53 negative), which were cotransfected with p53 and G9a or GLP. As shown in Figure 4, compound **5** at 0.25 μM effectively inhibited the dimethylation of p53 K373 without significant changes to levels of total p53 and G9a or GLP in H1299 cells. These results together with our previous H3K9me2 findings[34] strongly suggest that compound **5** is an effective inhibitor that blocks the methyltransferase activity of G9a and GLP in cells.

CONCLUSIONS

To improve cellular potency of the quinazoline series, we designed several generations of novel analogues aimed at achieving balanced G9a in vitro potency and physicochemical properties aiding cell penetration. New synthetic routes to efficiently synthesize these novel compounds were developed. SAR studies of these newly synthesized compounds in the G9a biochemical (SAHH-coupled), cell-based functional (anti-H3K9me2 ICW), and cell toxicity (MTT) assays validated our inhibitor design strategy and resulted in the discovery of compounds **6** and **7**, which had high cellular potency and excellent separation of functional potency versus cell toxicity in a variety of cell lines. Compounds **6** and **7** together with compound **5**, the previously reported G9a chemical probe, are valuable small molecule tools for the biomedical research community to further investigate the biology of G9a and its role in chromatin remodeling as well as PTMs of other proteins.

EXPERIMENTAL SECTION

Chemistry General Procedures. HPLC spectra for all compounds were acquired using an Agilent 6110 series system with UV detector set to 254 nm. Samples were injected (5 μL) onto an Agilent Eclipse Plus 4.6 mm × 50 mm, 1.8 μM, C18 column at room temperature. A linear gradient from 10% to 100% B (MeOH + 0.1% acetic acid) in 5.0 min was followed by pumping 100% B for another 2 min with A being H_2O + 0.1% acetic acid. The flow rate was 1.0 mL/min. Mass spectra (MS) data were acquired in positive ion mode using an Agilent 6110 single quadrupole mass spectrometer with an electrospray

dx.doi.org/10.1021/jm200903z | J. Med. Chem. 2011, 54, 6139–6150

ionization (ESI) source. High-resolution mass spectra (HRMS) were acquired using a Shimadzu LCMS-IT-TOF time-of-flight mass spectrometer. Nuclear magnetic resonance (NMR) spectra were recorded at Varian Mercury spectrometer with 400 MHz for proton (^{1}H NMR) and 100 MHz for carbon (^{13}C NMR); chemical shifts are reported in ppm (δ).[36] Preparative HPLC was performed on Agilent Prep 1200 series with UV detector set to 220 nm. Samples were injected onto a Phenomenex Luna 75 mm × 30 mm, 5 μM, C18 column at room temperature. The flow rate was 30 mL/min. A linear gradient was used with 10% of MeOH (A) in 0.1% TFA in H_2O (B) to 100% of MeOH (A). All compounds that were evaluated in biological assays had >95% purity using the HPLC methods described above.

2,4-Dichloro-6-methoxy-7-(3-(pyrrolidin-1-yl)propoxy)quinazoline (16). A solution of compound **13** (3.6 g, 11.67 mmol) (prepared from commercially available methyl 3-methoxy-4-hydroxy benzoate (**10**) according to the procedures described previously[34]) in acetic acid (20 mL) and water (10 mL) was treated with sodium cyanate (1.14 g, 17.5 mmol) while stirring, and then the mixture was stirred overnight at rt. After the resulting mixture was concentrated, the desired crude product **14** was obtained as a brown slurry oil. MS (ESI): 352 $[M + H]^+$. A mixture of crude compound **14** in MeOH (30 mL) was neutralized with 10% NaOH aqueous solution, and then an additional 10% NaOH aqueous solution (10 mL) was added. The mixture was refluxed for 3 h, cooled to room temperature, and neutralized with concentrated HCl to give a precipitate. The resulting precipitate was collected and dried to provide the desired crude product **15** (2.60 g). MS (ESI): 320 $[M + H]^+$. A mixture of the crude compound **15** (2.60 g, 8.14 mmol) and *N*,*N*-diethylaniline (1.3 mL, 8.14 mmol) in $POCl_3$ (45 mL) was heated at reflux for 7 h. The reaction mixture was concentrated in vacuo and saturated aq $NaHCO_3$ (50 mL) was added. The resulting mixture was extracted with chloroform (30 mL × 3). The combined organic layers were dried, concentrated, and purified by flash column chromatography on silica gel (0−20% MeOH/CH_2Cl_2) to afford the title compound **16** as a yellow solid (2.06 g, 50% over three steps). ^{1}H NMR (400 MHz, $CDCl_3$) δ 7.30 (s, 1H), 7.25 (s, 1H), 4.26 (t, J = 6.5 Hz, 2H), 4.02 (s, 3H), 2.74 (t, J = 7.3 Hz, 2H), 2.64 (m, 4H), 2.23−2.15 (m, 2H), 1.87−1.79 (m, 4H). MS (ESI): 356 $[M + H]^+$.

***N*-(1-Isopropylpiperidin-4-yl)-6-methoxy-2-(4-methyl-1,4-diazepan-1-yl)-7-(3-(pyrrolidin-1-yl)propoxy)quinazolin-4-amine (17a).** A mixture of compound **16** (0.72 g, 2.02 mmol), 1-isopropylpiperidin-4-amine (0.87 g, 6.06 mmol) (this amine and other noncommercially available amines were prepared according to the literature procedures[37]), and DIEA (0.67 mL, 4.04 mmol) in THF (10 mL) was stirred overnight at rt. After concentration in vacuo, the crude product was purified by silica gel chromatography (0−20% MeOH (1% NH_3)/CH_2Cl_2) to afford the desired product 2-chloro-*N*-(1-isopropylpiperidin-4-yl)-6-methoxy-7-(3-(pyrrolidin-1-yl)propoxy)quinazolin-4-amine as a yellow solid (0.88 g, 94% yield). ^{1}H NMR (400 MHz, $CDCl_3$) δ 7.12 (s, 1H), 6.78 (s, 1H), 5.36 (d, J = 7.7 Hz, 1H), 4.31−4.20 (m, 1H), 4.17 (t, J = 6.7 Hz, 2H), 3.96 (s, 3H), 2.90 (d, J = 11.9 Hz, 2H), 2.84−2.73 (m, 1H), 2.67−2.59 (m, 2H), 2.57−2.46 (m, 4H), 2.45−2.34 (m, 2H), 2.22−2.05 (m, 4H), 1.84−1.71 (m, 4H), 1.65−1.55 (m, 2H), 1.07 (d, J = 6.6 Hz, 6H). MS (ESI): 462 $[M + H]^+$. Then, a mixture of the intermediate (71 mg, 0.149 mmol), 1-methylhomopiperazine (34 mg, 0.30 mmol), and TFA (68 mg, 0.60 mmol) in *i*-PrOH (0.25 mL) was heated by microwave irradiation to 160 °C for 15 min in a sealed tube. After concentration in vacuo, the crude product was purified by preparative HPLC with a gradient from 10% of MeOH (A) in 0.1% TFA in H_2O (B) to 100% of MeOH (A). The resulting product was basified with saturated aq $NaHCO_3$ and extracted with CH_2Cl_2 to afford the title compound **17a** as a white solid (64 mg, 79% yield). ^{1}H NMR (400 MHz, $CDCl_3$) δ 6.87 (s, 1H), 6.71 (s, 1H), 4.98 (d, J = 7.1 Hz, 1H), 4.13 (t, J = 6.8 Hz, 2H), 4.08−3.98 (m, 1H), 3.97−3.92 (m, 2H), 3.89−3.82 (m, 5H), 2.91−2.84 (m, 2H), 2.78−2.69 (m, 1H), 2.69−2.63 (m, 2H), 2.61−2.56 (m, 2H), 2.55−2.50 (m, 2H), 2.51−2.44 (m, 4H), 2.34 (s, 3H), 2.29 (td, J = 11.5, 2.2 Hz, 2H), 2.19−2.11 (m, 2H), 2.11−2.02 (m, 2H), 2.01−1.94 (m, 2H), 1.79−1.70 (m, 4H), 1.54 (ddd, J = 14.9, 11.8, 3.7 Hz, 2H), 1.04 (d, J = 6.6 Hz, 6H). ^{13}C NMR (100 MHz, $CDCl_3$, two overlapping peaks) δ 158.70, 158.10, 154.05, 149.76, 145.22, 107.08, 102.79, 101.67, 67.40, 59.07, 57.46, 56.76, 54.58, 54.25, 53.01, 48.77, 47.88, 46.83, 45.98, 32.75, 28.64, 27.98, 23.56, 18.60. HPLC: 97%; t_R 1.18 min. MS (ESI): 540 $[M + H]^+$.

2-(4-Ethyl-1,4-diazepan-1-yl)-*N*-(1-isopropylpiperidin-4-yl)-6-methoxy-7-(3-(pyrrolidin-1-yl)propoxy)quinazolin-4-amine (17b). Compound **17b** was prepared as a white solid by the same procedures as the preparation of compound **17a** (80% yield). ^{1}H NMR (400 MHz, $CDCl_3$) δ 6.89 (s, 1H), 6.71 (s, 1H), 4.95 (d, J = 7.1 Hz, 1H), 4.15 (t, J = 6.8 Hz, 2H), 4.10−4.01 (m, 1H), 3.98−3.92 (m, 2H), 3.90−3.82 (m, 5H), 2.94−2.85(m, 2H), 2.80−2.71 (m, 3H), 2.64−2.46 (m, 10H), 2.36−2.26 (m, 2H), 2.20−2.13 (m, 2H), 2.12−2.04 (m, 2H), 2.02−1.93 (m, 2H), 1.82−1.70 (m, 4H), 1.56 (ddd, J = 14.6, 12.0, 3.5 Hz, 2H), 1.13−0.99 (m, 9H). ^{13}C NMR (100 MHz, $CDCl_3$) δ 158.75, 158.15, 154.10, 149.80, 145.26, 107.12, 102.81, 101.69, 67.43, 56.84, 55.94, 54.64, 54.47, 54.30, 53.08, 51.71, 48.76, 47.92, 46.28, 45.88, 32.77, 28.68, 27.97, 23.60, 18.63, 12.51. HPLC: 97%; t_R 1.14 min. MS (ESI): 554 $[M + H]^+$.

2-(4-Isopropyl-1,4-diazepan-1-yl)-*N*-(1-isopropylpiperidin-4-yl)-6-methoxy-7-(3-(pyrrolidin-1-yl)propoxy)quinazolin-4-amine (17c). Compound **17c** was prepared as an off-white solid by the same procedures as the preparation of compound **17a** (82% yield). ^{1}H NMR (400 MHz, $CDCl_3$) δ 6.87 (s, 1H), 6.72 (s, 1H), 4.98 (d, J = 7.1 Hz, 1H), 4.13 (t, J = 6.8 Hz, 2H), 4.09−3.99 (m, 1H), 3.93−3.87 (m, 2H), 3.88−3.80 (m, 5H), 2.95−2.83 (m, 3H), 2.78−2.69 (m, 3H), 2.62−2.53 (m, 4H), 2.53−2.43 (m, 4H), 2.33−2.23 (m, 2H), 2.20−2.11 (m, 2H), 2.10−2.02 (m, 2H), 1.94−1.85 (m, 2H), 1.81−1.68 (m, 4H), 1.54 (ddd, J = 14.6, 12.0, 3.6 Hz, 2H), 1.04 (d, J = 6.6 Hz, 6H), 0.98 (d, J = 6.5 Hz, 6H). ^{13}C NMR (100 MHz, $CDCl_3$, two overlapping peaks) δ 158.74, 158.14, 154.00, 149.85, 145.12, 107.08, 102.78, 101.72, 67.39, 56.77, 55.20, 54.57, 54.25, 53.02, 52.26, 50.68, 48.76, 47.89, 47.80, 45.77, 32.76, 28.78, 28.65, 23.56, 18.61. HPLC: 99%; t_R 1.25 min. MS (ESI): 568 $[M + H]$.

2-(4-Cyclohexyl-1,4-diazepan-1-yl)-*N*-(1-isopropylpiperidin-4-yl)-6-methoxy-7-(3-(pyrrolidin-1-yl)propoxy)quinazolin-4-amine (17d). Compound **17d** was prepared as a white solid by the same procedures as the preparation of compound **17a** (78% yield). ^{1}H NMR (400 MHz, $CDCl_3$) δ 6.87 (s, 1H), 6.72 (s, 1H), 4.98 (d, J = 7.1 Hz, 1H), 4.13 (t, J = 6.8 Hz, 2H), 4.09−3.97 (m, 1H), 3.92−3.78 (m, 7H), 2.91−2.84 (m, 2H), 2.83−2.77 (m, 2H), 2.77−2.68 (m, 1H), 2.65−2.60 (m, 2H), 2.58 (t, J = 7.4 Hz, 2H), 2.53−2.39 (m, 5H), 2.33−2.24 (m, 2H), 2.18−2.10 (m, 2H), 2.10−2.00 (m, 2H), 1.92−1.83 (m, 2H), 1.82−1.68 (m, 8H), 1.62−1.47 (m, 3H), 1.25−1.06 (m, 5H), 1.04 (d, J = 6.5 Hz, 6H). ^{13}C NMR (100 MHz, $CDCl_3$) δ 158.73, 158.13, 153.98, 149.86, 145.09, 107.07, 102.76, 101.72, 67.37, 64.43, 56.75, 54.56, 54.24, 53.01, 52.64, 51.26, 48.75, 47.99, 47.89, 45.78, 32.75, 29.34, 28.85, 28.64, 26.49, 26.19, 23.55, 18.60. HPLC: 99%; t_R 2.16 min. MS (ESI): 608 $[M + H]^+$.

2-(4-(Cyclohexylmethyl)-1,4-diazepan-1-yl)-*N*-(1-isopropylpiperidin-4-yl)-6-methoxy-7-(3-(pyrrolidin-1-yl)propoxy)quinazolin-4-amine (17e). Compound **17e** was prepared as a white solid by the same procedures as the preparation of compound **17a** (81% yield). ^{1}H NMR (400 MHz, $CDCl_3$) δ 6.87 (s, 1H), 6.73 (s, 1H), 4.99 (d, J = 7.1 Hz, 1H), 4.13 (t, J = 6.8 Hz, 2H), 4.09−3.98 (m, 1H), 3.94−3.87 (m, 2H), 3.87−3.76 (m, 5H), 2.91−2.83 (m, 2H), 2.78−2.67 (m, 3H), 2.62−2.52 (m, 4H), 2.52−2.43 (m, 4H), 2.29 (t, J = 10.7 Hz, 2H), 2.22 (d, J = 6.9 Hz, 2H), 2.15 (d, J = 10.8 Hz, 2H), 2.11−2.01 (m, 2H), 1.96−1.86 (m, 2H), 1.81−1.48 (m, 11H), 1.47−1.34 (m, 1H), 1.26−1.10 (m, 3H), 1.04 (d, J = 6.5 Hz, 6H), 0.88−0.74 (m, 2H). ^{13}C NMR (100 MHz, $CDCl_3$, two overlapping peaks) δ 158.75, 158.10, 153.99, 149.86, 145.10, 107.07, 102.76, 101.72, 67.38, 64.33, 56.75, 55.34, 54.56, 54.24, 53.01, 48.77, 47.89, 46.62, 45.96, 36.32, 32.74, 32.00, 28.64, 27.93, 26.96, 26.30, 23.56, 18.60. HPLC: 99%; t_R 2.39 min. MS (ESI): 622 $[M + H]^+$.

***N*-(1-Isopropylpiperidin-4-yl)-6-methoxy-2-(4-phenyl-1,4-diazepan-1-yl)-7-(3-(pyrrolidin-1-yl)propoxy)quinazolin-4-amine (17f).** Compound **17f** was prepared as a yellow solid by the same procedures as the preparation of compound **17a** (74% yield). ^{1}H NMR (400 MHz, $CDCl_3$) δ 7.22 (t, J = 7.9 Hz, 2H), 6.90 (s, 1H), 6.80−6.72 (m, 3H), 6.65 (t, J = 7.2 Hz, 1H), 4.99 (d, J = 7.1 Hz, 1H), 4.18 (t, J = 6.8 Hz, 2H), 4.14−3.99 (m, 3H), 3.90 (s, 3H), 3.71−3.61 (m, 4H), 3.51 (t, J = 6.2 Hz, 2H), 2.96−2.87 (m, 2H), 2.83−2.70 (m, 1H), 2.62 (t, J = 7.3 Hz, 2H), 2.58− 2.45 (m, 4H), 2.32 (t, J = 10.7 Hz, 2H), 2.22−2.05 (m, 6H), 1.85−1.72 (m, 4H), 1.58 (ddd, J = 14.7, 11.9, 3.5 Hz, 2H), 1.08 (d, J = 6.5 Hz, 6H). ^{13}C NMR (100 MHz, $CDCl_3$) δ 158.40, 158.31, 154.12, 149.87, 147.69, 145.37, 129.52, 115.76, 111.66, 107.14, 102.93, 101.63, 67.42, 56.81, 54.60, 54.29, 53.06, 50.56, 48.83, 47.93, 47.78, 47.10, 46.12, 32.86, 28.67, 24.89, 23.59, 18.61. HPLC: 98%; t_R 3.29 min. MS (ESI): 602 $[M + H]^+$.

2-(4-Benzyl-1,4-diazepan-1-yl)-*N*-(1-isopropylpiperidin-4-yl)-6-methoxy-7-(3-(pyrrolidin-1-yl)propoxy)quinazolin-4-amine (17g). Compound **17g** was prepared as an off-white solid by the same procedures as the preparation of compound **17a** (78% yield). ^{1}H NMR (400 MHz, $CDCl_3$) δ 7.25−7.12 (m, 5H), 6.82 (s, 1H), 6.67 (s, 1H), 4.95 (d, J = 7.0 Hz, 1H), 4.08 (t, J = 6.8 Hz, 2H), 4.02−3.91 (m, 1H), 3.90−3.84 (m, 2H), 3.84−3.75 (m, 5H), 3.55 (s, 2H), 2.87−2.77 (m, 2H), 2.74−2.61 (m, 3H), 2.59−2.50 (m, 4H), 2.47−2.38 (m, 4H), 2.21 (t, J = 11.3 Hz, 2H), 2.15−1.95 (m, 4H), 1.94−1.83 (m, 2H), 1.73−1.63 (m, 4H), 1.48 (ddd, J = 14.6, 11.9, 3.5 Hz, 2H), 0.98 (d, J = 6.5 Hz, 6H). ^{13}C NMR (100 MHz, $CDCl_3$) δ 158.71, 158.12, 154.04, 149.76, 145.19, 139.61, 128.91, 128.20, 126.87, 107.06, 102.79, 101.72, 67.39, 62.30, 56.76, 56.28, 54.98, 54.58, 54.25, 53.02, 48.76, 47.87, 46.58, 46.01, 32.72, 28.63, 28.15, 23.56, 18.58. HPLC: 98%; t_R 2.27 min. MS (ESI): 616 $[M + H]^+$.

***N*-(1-Isopropylpiperidin-4-yl)-6-methoxy-2-(piperidin-1-yl)-7-(3-(pyrrolidin-1-yl)propoxy)quinazolin-4-amine (17h).** Compound **17h** was prepared as a white solid by the same procedures as the preparation of compound **17a** (76% yield). ^{1}H NMR (400 MHz, $CDCl_3$) δ 6.90 (s, 1H), 6.75 (s, 1H), 5.10 (d, J = 7.2 Hz, 1H), 4.21−4.01 (m, 3H), 3.87 (s, 3H), 3.80−3.73 (m, 4H), 2.98−2.86 (m, 2H), 2.82−2.72 (m, 1H), 2.65−2.57 (m, 2H), 2.58−2.45 (m, 4H), 2.40−2.28 (m, 2H), 2.20−2.12 (m, 2H), 2.12−2.02 (m, 2H), 1.82−1.69 (m, 4H), 1.69−1.53 (m, 8H), 1.07 (d, J = 6.6 Hz, 6H). ^{13}C NMR (100 MHz, $CDCl_3$) δ 158.95, 158.27, 154.01, 149.36, 145.46, 106.97, 102.93, 101.65, 67.35, 56.71, 54.74, 54.24, 53.02, 48.48, 47.89, 45.18, 32.47, 28.54, 26.07, 25.19, 23.56, 18.51. HPLC: 97%; t_R 2.92 min. MS (ESI): 511 $[M + H]^+$.

2-(Azepan-1-yl)-*N*-(1-isopropylpiperidin-4-yl)-6-methoxy-7-(3-(pyrrolidin-1-yl)propoxy)quinazolin-4-amine (17i). Compound **17i** was prepared as a white solid by the same procedures as the preparation of compound **17a** (78% yield). ^{1}H NMR (400 MHz, $CDCl_3$) δ 6.89 (s, 1H), 6.72 (s, 1H), 4.96 (d, J = 6.9 Hz, 1H), 4.15 (t, J = 6.8 Hz, 2H), 4.11−4.00 (m, 1H), 3.87 (s, 3H), 3.77 (t, J = 5.9 Hz, 4H), 2.93−2.85 (m, 2H), 2.80−2.68 (m, 1H), 2.60 (t, J = 7.4 Hz, 2H), 2.55−2.44 (m, 4H), 2.35−2.24 (m, 2H), 2.17 (d, J = 11.3 Hz, 2H), 2.13−2.02 (m, 2H), 1.85−1.67 (m, 8H), 1.63−1.47 (m, 6H), 1.05 (d, J = 6.5 Hz, 6H). ^{13}C NMR (100 MHz, $CDCl_3$) δ 158.76, 158.15, 154.03, 149.91, 145.04, 107.06, 102.71, 101.81, 67.41, 56.84, 54.61, 54.29, 53.06, 48.83, 47.94, 46.99, 32.82, 28.69, 28.66, 27.53, 23.59, 18.62. HPLC: 98%; t_R 3.09 min. MS (ESI): 525 $[M + H]^+$.

7-(Benzyloxy)-2-cyclohexyl-6-methoxyquinazolin-4(3*H*)-one (20). Cyclohexanecarbonyl chloride (1.25 mL, 9.2 mmol) was added into a solution of compound **19** (1.95 g, 7.64 mmol) (prepared from commercially available 4-hydroxy-3-methoxybenzonitrile (**18**) according to the procedures described previously[31,32]) and DIEA (1.90 mL, 11.5 mmol) in cosolvent DMF:DCM (10 mL:5 mL) at 0 °C. The reaction mixture was stirred overnight at rt, 25 mL of water was added, and the resulting mixture was extracted with CH_2Cl_2 (15 mL × 3). The combined organic solvent was dried with sodium sulfate, concentrated, and used in the next step without further purification. A mixture of the product, 30 wt % H_2O_2 (20 mL) and NaOH (400 mg, 10.0 mmol) in ethanol (100 mL) was stirred for 2 h under reflux. After adding 100 mL of water, the reaction mixture was cooled to rt and the resulting precipitate was collected, washed with water, and dried to afford the title compound **20** as a white solid (1.35 g, 48% yield over 2 steps). ^{1}H NMR (400 MHz, $CDCl_3$) δ 9.63 (s, 1H), 7.60 (s, 1H), 7.50−7.30 (m, 5H), 7.15 (s, 1H), 5.26 (s, 2H), 3.99 (s, 3H), 2.66−2.53 (m, 1H), 2.03 (d, J = 12.2 Hz, 2H), 1.96−1.86 (m, 2H), 1.83−1.74 (m, 1H), 1.68−1.52 (m, 2H), 1.49−1.24 (m, 3H).

7-(Benzyloxy)-4-chloro-2-cyclohexyl-6-methoxyquinazoline (21). A mixture of the compound **20** (1.32 g, 3.61 mmol) and *N*,*N*-diethylaniline (0.30 mL, 1.80 mmol) in $POCl_3$ (20 mL) was heated at reflux for 4 h. The reaction mixture was concentrated in vacuo, and saturated aq $NaHCO_3$ (20 mL) was added. The resulting mixture was extracted with chloroform (20 mL × 3). The combined organic layers were dried, concentrated, and purified by flash column chromatography on silica gel (0−10% ethyl acetate/hexanes) to afford the title compound **21** as a yellow solid (1.10 g, 79% yield). ^{1}H NMR (400 MHz, $CDCl_3$) δ 7.51−7.30 (m, 7H), 5.30 (s, 2H), 4.04 (s, 3H), 2.92 (tt, J = 11.7, 3.4 Hz, 1H), 2.10−1.99 (m, 2H), 1.93−1.84 (m, 2H), 1.79−1.64 (m, 3H), 1.49−1.27 (m, 3H).

7-(Benzyloxy)-2-cyclohexyl-*N*-(1-isopropylpiperidin-4-yl)-6-methoxyquinazolin-4-amine (22). A mixture of compound **21** (0.68 g, 1.77 mmol), 1-isopropylpiperidin-4-amine (0.77 g, 5.41 mmol), and DIEA (0.60 mL, 3.60 mmol) in *i*-PrOH (3.0 mL) was heated by microwave irradiation to 160 °C for 15 min in a sealed tube. After concentration in vacuo, the crude product was purified by silica gel chromatography (0−10% MeOH/CH_2Cl_2) to afford the title compound **22** as a white solid (0.81 g, 94% yield). ^{1}H NMR (400 MHz, MeOH-d_4) δ 7.52 (s, 1H), 7.45 (d, J = 7.2 Hz, 2H), 7.34 (t, J = 7.3 Hz, 2H), 7.31−7.24 (m, 1H), 7.11 (s, 1H), 5.18 (s, 2H), 4.27−4.19 (m, 1H), 3.94 (s, 3H), 2.98 (d, J = 11.7 Hz, 2H), 2.81−2.71 (m, 1H), 2.69−2.57 (m, 1H), 2.35 (t, J = 11.4 Hz, 2H), 2.13 (d, J = 11.4 Hz, 2H), 1.91−1.82 (m, 4H), 1.79−1.61 (m, 5H), 1.49−1.23 (m, 3H), 1.10 (d, J = 6.5 Hz, 6H). MS (ESI): 489 $[M + H]^+$.

2-Cyclohexyl-*N*-(1-isopropylpiperidin-4-yl)-6-methoxy-7-(3-(pyrrolidin-1-yl)propoxy)quinazolin-4-amine (5). A mixture of compound **22** (0.81 g, 1.65 mmol), 1,4-cyclohexadiene (1.6 mL, 16.5 mmol), and 10 wt % Pd/C (250 mg) in ethanol (16 mL) was heated to reflux 2 h. The reaction mixture was filtered and concentrated to provide the debenzylated product **23** as a yellow solid which was used without purification. MS (ESI): 399 $[M + H]^+$. Under nitrogen gas, DIAD (270 μL, 1.38 mmol) was added into an ice-cooled mixture of compound **21** (110 mg, 0.276 mmol), 3-(pyrrolidin-1-yl)propan-1-ol (142 mg, 1.10 mmol), and PPh_3 (399 mg, 1.52 mmol) in THF (4.0 mL). The reaction mixture was stirred overnight at rt. After concentration in vacuo, the crude product was purified by preparative HPLC with a gradient from 10% of MeOH (A) in 0.1% TFA in H_2O (B) to 100% of MeOH (A). The resulting product was basified with a saturated solution of $NaHCO_3$ and extracted with CH_2Cl_2 to afford 56 mg of the desired product **5** as a white solid (91 mg, 65% yield over 2 steps). The characterization data (^{1}H and ^{13}C NMR, HPLC, HRMS) of the title compound match the reported.[34]

2-Cyclohexyl-*N*-(1-isopropylpiperidin-4-yl)-6-methoxy-7-(3-(piperidin-1-yl)propoxy)quinazolin-4-amine (24a). Compound **24a** was prepared as a white solid from compound **23** and 3-(piperidin-1-yl)propan-1-ol via Mitsunobu reaction (52% over two steps). ^{1}H NMR (400 MHz, $CDCl_3$) δ 7.13 (s, 1H), 6.82 (s, 1H), 5.22 (d, J = 7.3 Hz, 1H), 4.25−4.07 (m, 3H), 3.88 (s, 3H), 2.93−2.84(m, 2H), 2.81−2.63 (m, 2H), 2.48−2.25 (m, 8H), 2.19 (d, J = 11.3 Hz, 2H), 2.08−1.90 (m, 4H), 1.81 (d, J = 12.6 Hz, 2H), 1.75−1.47 (m, 9H), 1.47−1.17 (m, 5H), 1.05 (d, J = 6.5 Hz, 6H). ^{13}C NMR (100 MHz, $CDCl_3$) δ 169.44, 157.93, 153.68, 148.40, 147.38, 108.51, 106.73, 100.07, 67.73, 56.43, 55.78, 54.64, 54.62, 48.59, 47.97, 47.85, 32.67, 32.01, 26.49, 26.48, 26.32, 26.08, 24.53, 18.56. HPLC: 99%; t_R 3.10 min. MS (ESI): 524 $[M + H]^+$.

2-Cyclohexyl-7-(2-(2-(dimethylamino)ethoxy)ethoxy)-*N*-(1-isopropylpiperidin-4-yl)-6-methoxyquinazolin-4-amine (24b). Compound **24b** was prepared as a white solid from compound **23** and

2-(2-(dimethylamino)ethoxy)ethanol via Mitsunobu reaction (36% over two steps). ^{1}H NMR (400 MHz, $CDCl_3$) δ 7.11 (s, 1H), 6.83 (s, 1H), 5.22 (d, J = 7.2 Hz, 1H), 4.27−4.13 (m, 3H), 3.92−3.83 (m, 5H), 3.61 (t, J = 5.8 Hz, 2H), 2.93−2.85 (m, 2H), 2.80−2.64 (m, 2H), 2.48 (t, J = 5.8 Hz, 2H), 2.40−2.31 (m, 2H), 2.22 (s, 6H), 2.19 (d, J = 10.5 Hz, 2H), 1.95 (d, J = 11.9 Hz, 2H), 1.86−1.76 (m, 2H), 1.75−1.50 (m, 5H), 1.46−1.21 (m, 3H), 1.05 (d, J = 6.5 Hz, 6H). ^{13}C NMR (100 MHz, $CDCl_3$) δ 169.49, 157.94, 153.43, 148.39, 147.26, 108.52, 107.00, 100.20, 69.62, 69.01, 68.19, 58.84, 56.39, 54.61, 48.62, 47.98, 47.86, 45.91, 32.67, 32.01, 26.49, 26.32, 18.58. HPLC: 99%; t_R 2.98 min. MS (ESI): 514 $[M + H]^+$.

***N*-(1-Cyclohexylpiperidin-4-yl)-2-(4-isopropyl-1,4-diazepan-1-yl)-6-methoxy-7-(3-(piperidin-1-yl)propoxy)quinazolin-4-amine (6).** Compound **6** was prepared as a white solid by the same procedures as the preparation of compound **17a** (81% yield). ^{1}H NMR (400 MHz, $CDCl_3$) δ 6.87 (s, 1H), 6.72 (s, 1H), 4.99 (d, J = 7.1 Hz, 1H), 4.11 (t, J = 6.8 Hz, 2H), 4.08−3.98 (m, 1H), 3.93−3.88 (m, 2H), 3.87−3.78 (m, 5H), 3.17−3.00 (m, 1H), 2.96−2.85 (m, 3H), 2.78−2.70 (m, 2H), 2.60−2.52 (m, 2H), 2.49−2.23 (m, 8H), 2.14 (d, J = 11.1 Hz, 2H), 2.07−1.98 (m, 2H), 1.94−1.71 (m, 6H), 1.66−1.47 (m, 7H), 1.45−1.35 (m, 2H), 1.22 (p, J = 11.7 Hz, 4H), 1.15−1.03 (m, 1H), 0.98 (d, J = 6.6 Hz, 6H). ^{13}C NMR (100 MHz, $CDCl_3$) δ 158.75, 158.12, 154.00, 149.85, 145.12, 107.05, 102.78, 101.72, 67.50, 63.86, 56.75, 55.86, 55.20, 54.66, 52.27, 50.69, 48.82, 48.27, 47.78, 45.77, 32.90, 29.05, 28.79, 26.59, 26.47, 26.14, 26.10, 24.56, 18.61. HPLC: 100%; t_R 2.25 min. MS (ESI): 622 $[M + H]^+$. HRMS (ESI) calcd for $C_{36}H_{60}N_7O_2$ $[M + H]^+$, 622.4808; found, 622.4810.

***N*-(1-(Cyclohexylmethyl)piperidin-4-yl)-2-(4-isopropyl-1,4-diazepan-1-yl)-6-methoxy-7-(3-(piperidin-1-yl)propoxy)quinazolin-4-amine (7).** Compound **7** was prepared as a white solid by the same procedures as the preparation of compound **17a** (81% yield). ^{1}H NMR (400 MHz, $CDCl_3$) δ 6.88 (s, 1H), 6.72 (s, 1H), 4.97 (d, J = 6.9 Hz, 1H), 4.13 (t, J = 6.8 Hz, 2H), 4.10−4.00 (m, 1H), 3.94−3.88 (m, 2H), 3.88−3.79 (m, 5H), 2.97−2.88 (m, 1H), 2.88−2.81 (m, 2H), 2.80−2.71 (m, 2H), 2.62−2.54 (m, 2H), 2.50−2.42 (m, 2H), 2.41−2.32 (m, 4H), 2.19−1.98 (m, 8H), 1.96−1.85 (m, 2H), 1.82−1.36 (m, 14H), 1.30−1.09 (m, 3H), 0.99 (d, J = 6.6 Hz, 6H), 0.93−0.80 (m, 2H). ^{13}C NMR (100 MHz, $CDCl_3$) δ 158.79, 158.16, 154.05, 149.87, 145.17, 107.11, 102.81, 101.69, 67.55, 65.89, 56.78, 55.90, 55.23, 54.70, 53.30, 52.28, 50.73, 48.59, 47.80, 45.79, 35.57, 32.45, 32.10, 28.82, 26.95, 26.64, 26.31, 26.15, 24.61, 18.65. HPLC: 99%; t_R 2.56 min. MS (ESI): 636 $[M + H]^+$. HRMS (ESI) calcd for $C_{37}H_{62}N_7O_2$ $[M + H]^+$, 636.4965; found, 636.4962.

2-(4-Isopropyl-1,4-diazepan-1-yl)-*N*-(1-isopropylpiperidin-4-yl)-6-methoxy-7-(3-(piperidin-1-yl)propoxy)quinazolin-4-amine (25). Compound **25** was prepared as a white solid by the same procedures as the preparation of compound **17a** (78% yield). ^{1}H NMR (400 MHz, $CDCl_3$) δ 6.87 (s, 1H), 6.72 (s, 1H), 4.98 (d, J = 7.1 Hz, 1H), 4.12 (t, J = 6.8 Hz, 2H), 4.09−3.99 (m, 1H), 3.95−3.88 (m, 2H), 3.88−3.78 (m, 5H), 2.97−2.83 (m, 3H), 2.78−2.68 (m, 3H), 2.60−2.53 (m, 2H), 2.49−2.40 (m, 2H), 2.40−2.24 (m, 6H), 2.15 (d, J = 11.1 Hz, 2H), 2.08−1.98 (m, 2H), 1.96−1.84 (m, 2H), 1.61−1.48 (m, 6H), 1.45−1.36 (m, 2H), 1.05 (d, J = 6.5 Hz, 6H), 0.98 (d, J = 6.5 Hz, 6H). ^{13}C NMR (100 MHz, $CDCl_3$, two overlapping peaks) δ 158.76, 158.14, 154.03, 149.86, 145.14, 107.07, 102.77, 101.74, 67.51, 56.77, 55.87, 55.21, 54.67, 54.58, 52.28, 50.70, 48.76, 47.90, 47.80, 45.78, 32.77, 28.80, 26.60, 26.11, 24.57, 18.61. HPLC: 98%; t_R 1.40 min. MS (ESI): 582 $[M + H]^+$.

***N*-(1-Cyclohexylpiperidin-4-yl)-6-methoxy-2-(4-methyl-1,4-diazepan-1-yl)-7-(3-(piperidin-1-yl)propoxy)quinazolin-4-amine (26).** Compound **26** was prepared as a white solid by the same procedures as the preparation of compound **17a** (83% yield). ^{1}H NMR (400 MHz, $CDCl_3$) δ 6.87 (s, 1H), 6.72 (s, 1H), 5.03 (d, J = 7.1 Hz, 1H), 4.11 (t, J = 6.8 Hz, 2H), 4.07−3.98 (m, 1H), 3.97−3.90 (m, 2H), 3.88−3.79 (m, 5H), 3.27−3.08 (m, 1H), 2.96−2.86 (m, 2H), 2.70−2.62 (m, 2H), 2.58−2.50 (m, 2H), 2.48−2.24 (m, 11H), 2.13 (d, J = 11.0 Hz, 2H), 2.06−1.93 (m, 4H), 1.90−1.71 (m, 4H), 1.66−1.48 (m, 7H), 1.46−1.33 (m, 2H), 1.22 (p, J = 12.0 Hz, 4H), 1.13−1.00 (m, 1H). HPLC: 99%; t_R 2.26 min. MS (ESI): 594 $[M + H]^+$.

2-(Azepan-1-yl)-*N*-(1-isopropylpiperidin-4-yl)-6-methoxy-7-(3-(piperidin-1-yl)propoxy)quinazolin-4-amine (27). Compound **27** was prepared as a white solid by the same procedures as the preparation of compound **17a** (75% yield). ^{1}H NMR (400 MHz, $CDCl_3$) δ 6.88 (s, 1H), 6.72 (s, 1H), 4.95 (d, J = 7.0 Hz, 1H), 4.13 (t, J = 6.8 Hz, 2H), 4.10−4.00 (m, 1H), 3.87 (s, 3H), 3.78 (t, J = 6.0 Hz, 4H), 2.93−2.85 (m, 2H), 2.80−2.68 (m, 1H), 2.50−2.42 (m, 2H), 2.41−2.24 (m, 6H), 2.17 (d, J = 10.8 Hz, 2H), 2.0−1.98 (m, 2H), 1.83−1.73 (m, 4H), 1.62−1.49 (m, 10H), 1.45−1.36 (m, 2H), 1.05 (d, J = 6.5 Hz, 6H). ^{13}C NMR (100 MHz, $CDCl_3$) δ 158.81, 158.15, 154.03, 149.98, 145.03, 107.06, 102.70, 101.80, 67.52, 56.82, 55.90, 54.68, 54.60, 48.82, 47.94, 46.97, 32.83, 28.67, 27.54, 26.63, 26.13, 24.59, 18.62. HPLC: 100%; t_R 3.06 min. MS (ESI): 539 $[M + H]^+$.

ALogP Calculation. ALogP values were calculated using Pipeline Pilot v7.5 (Accelrys Software Inc., San Diego, 2009).

Experimental Procedures for SAHH-Coupled Assays. The previously described enzyme-coupled assay[38] was optimized and employed to assay the activity of histone methyltransferases. This assay utilizes SAHH to hydrolyze the methyltransfer product SAH to homocysteine and adenosine in the presence of adenosine deaminase, which converts adenosine to inosine. The homocysteine concentration is then determined through conjugation of its free sulfhydryl moiety to a thiol-sensitive fluorophore, ThioGlo (Calbiochem). For IC_{50} determinations, assay mixtures were prepared in 25 mM potassium phosphate buffer pH 7.5, 1 mM EDTA, 2 mM $MgCl_2$, 0.01% Triton X-100 with 5 μM SAHH, 0.3 U/mL of adenosine deaminase from Sigma, 25 μM SAM, and 15 μM ThioGlo. G9a, GLP, SETD7, SETD8, PRMT3, and SUV39H2 were assayed at 25, 100, 200, 250, 500, and 100 nM, respectively. Inhibitors were added at concentrations ranging from 4 to 16 μM. After 2 min incubation, reactions were initiated by addition of the histone peptides: 10 μM H3(1−25) for G9a, 20 μM H3(1−25) for GLP, 100 μM H3(1−25) for SETD7, 500 μM H4(1−24) for SETD8, 10 μM H4(1−24) for PRMT3, and 200 μM H3K9Me1 (1−15) for SUV39H2. The methylation reaction was followed by monitoring the increase in fluorescence using Biotek Synergy2 plate reader with 360/40 nm excitation filter and 528/20 nm emission filter for 20 min in 384-well plate format. Activity values were corrected by subtracting background caused by the peptide or the protein. IC_{50} values were calculated using Sigmaplot. Standard deviations were calculated from two independent experiments.

Experimental Procedures for ICW and MTT Assays. MDA-MB-231, PC3, and HCT116 cells were cultured in RPMI with 10% FBS, 22RV1 cells in alphaMEM and 10% FBS, MCF7 and IMR90 cells in DMEM with 10% FBS. Cells were treated with inhibitors for 48 h.

In-Cell Western (ICW) Assay. Cells were seeded at 5000−10000 cells in black-walled 96-well plates (Greiner) and exposed to various inhibitor concentrations for 48 h. The media was removed and 2% formaldehyde in PBS for fixation was added for 15 min. After five washes with 0.1% Triton X100 in PBS, cells were blocked for 1 h with 1% BSA in PBS. Three out of four replicates were exposed to the primary H3K9me2 antibody, Abcam no. 1220 at 1/800 dilution in 1% BSA, PBS for 2 h. One replicate was reserved for the background control. The wells were washed five times with 0.1% Tween 20 in PBS, then secondary IR800 conjugated antibody (LiCor) and nucleic acid-intercalating dye, DRAQ5 (LiCor) added for 1 h. After 5 washes with 0.1% Tween 20 PBS, the plates were read on an Odyssey (LiCor) scanner at 800 nm (H3K9me2 signal) and 700 nm (DRAQ5 signal). Fluorescence intensity was quantified, normalized to the background, then to the DRAQ5 signal, and expressed as a percentage of control. IC_{50}s were calculated using GraphPad Prizm statistical package with sigmoidal variable slope dose response curve fit.

MTT Assay. The media was removed and replaced with DMEM 10% FBS without phenol red supplemented with 1 mg/mL of MTT and

incubated for 1−2 h. Live cells reduce yellow MTT to purple formazan. The resulting formazan was solubilized in acidified isopropyl alcohol and 1% Triton. Formazan signal absorbance was measured at 570 nm and corrected for the 650 nm background. The data was analyzed as above.

Experimental Procedures for the p53 K373me2 Assay. H1299 cells were transfected with 1 μg p53 expressing vector and 11 μg G9a or GLP expressing vector. Immediately after transfection, cells were treated with 0.25 μM of compound **5** and incubated for 24 h. Cells were then lysed in NET buffer (50 mM Tris-HCl, pH 8.0, 0.1% NP40, 5 mM EDTA, 150 mM NaCl with protease inhibitors) and followed by immunoprecipitation with DO1 antibody, which recognizing the total p53. Protein A agarose beads were added to collect the immunoprecipitated complex. The immunoprecipitated complex was subject to the Western blot analysis using p53 K373me2 antibody. For p53 and G9a/GLP detection, whole cell lysate was used.

■ ASSOCIATED CONTENT

Ⓢ Supporting Information. ^{1}H and ^{13}C NMR spectra of compounds **6** and **7**. This material is available free of charge via the Internet at http://pubs.acs.org.

■ AUTHOR INFORMATION

Corresponding Author

*Phone: 919-843-8459. Fax: 919-843-8465. E-mail: jianjin@unc.edu.

Present Addresses

[⊥]Viamet Pharmaceuticals, Inc., 2250 Perimeter Park Drive, Suite 320, Morrisville, North Carolina 27560, United States.

Author Contributions

[∥]These authors contributed equally to this work.

■ ACKNOWLEDGMENT

We thank Dr. Ryan Trump for helpful discussions, Dr. Cen Gao for ALogP calculation, and Dr. R. Bristow for 22RV1 and PC3 cells. The research described here was supported by the grant RC1GM090732 from the NIH, the Carolina Partnership and University Cancer Research Fund from the University of North Carolina at Chapel Hill, and the Structural Genomics Consortium, a registered charity (no. 1097737) that receives funds from the Canadian Institutes of Health Research, the Canada Foundation for Innovation, Genome Canada through the Ontario Genomics Institute, GlaxoSmithKline, Karolinska Institutet, the Knut and Alice Wallenberg Foundation, the Ontario Innovation Trust, the Ontario Ministry for Research and Innovation, Merck & Co., Inc., the Novartis Research Foundation, the Swedish Agency for Innovation Systems, the Swedish Foundation for Strategic Research and the Wellcome Trust.

■ ABBREVIATIONS USED

H3K9me2, dimethylation of lysine 9 on histone H3; SAR, structure−activity relationships; PTMs, post-translational modifications; PKMTs, protein lysine methyltransferases; SAM, *S*-adenosyl-L-methionine; SET, suppressor of variegation 3−9, enhancer of zeste, and trithorax; MBT domains, malignant brain tumor domains; PHD, plant homeo domain; KMT1C, lysine methyltransferase 1C; EHMT2, euchromatic histone lysine methyltransferase 2; H3K9, histone H3 lysine 9; p53 K373, lysine 373 of p53; KMT1D, lysine methyltransferase 1D; EHMT1, euchromatic histone lysine methyltransferase 1; ES cells, embryonic stem cells; tox/function ratio, ratio of toxicity to functional potency; SAHH, *S*-adenosyl-L-homocysteine hydrolase; ICW, in-cell western; MTT, 3-(4,5-dimethylthiazol-2-yl)-2,5-diphenyl tetrazolium bromide; PRMT, protein arginine methyltransferase; p53 K373me2, dimethylation of p53 lysine 373; SAH, *S*-adenosyl-L-homocysteine

■ REFERENCES

(1) Strahl, B. D.; Allis, C. D. The language of covalent histone modifications. *Nature* **2000**, *403*, 41–45.

(2) Jenuwein, T.; Allis, C. D. Translating the histone code. *Science* **2001**, *293*, 1074–80.

(3) Kouzarides, T. Chromatin modifications and their function. *Cell* **2007**, *128*, 693–705.

(4) Copeland, R. A.; Solomon, M. E.; Richon, V. M. Protein methyltransferases as a target class for drug discovery. *Nature Rev. Drug Discovery* **2009**, *8*, 724–732.

(5) Fog, C. K.; Jensen, K. T.; Lund, A. H. Chromatin-modifying proteins in cancer. *Acta Pathol. Microbiol. Immunol. Scand.* **2007**, *115*, 1060–1089.

(6) Rea, S.; Eisenhaber, F.; O'Carroll, D.; Strahl, B. D.; Sun, Z. W.; Schmid, M.; Opravil, S.; Mechtler, K.; Ponting, C. P.; Allis, C. D.; Jenuwein, T. Regulation of chromatin structure by site-specific histone H3 methyltransferases. *Nature* **2000**, *406*, 593–599.

(7) Ruthenburg, A. J.; Li, H.; Patel, D. J.; Allis, C. D. Multivalent engagement of chromatin modifications by linked binding modules. *Nature Rev. Mol. Cell Biol.* **2007**, *8*, 983–994.

(8) Wang, G. G.; Song, J.; Wang, Z.; Dormann, H. L.; Casadio, F.; Li, H.; Luo, J. L.; Patel, D. J.; Allis, C. D. Haematopoietic malignancies caused by dysregulation of a chromatin-binding PHD finger. *Nature* **2009**, *459*, 847–851.

(9) Fritsch, L.; Robin, P.; Mathieu, J. R.; Souidi, M.; Hinaux, H.; Rougeulle, C.; Harel-Bellan, A.; Ameyar-Zazoua, M.; Ait-Si-Ali, S. A subset of the histone H3 lysine 9 methyltransferases Suv39h1, G9a, GLP, and SETDB1 participate in a multimeric complex. *Mol. Cell* **2010**, *37*, 46–56.

(10) Frye, S. V. The art of the chemical probe. *Nature Chem. Biol.* **2010**, *6*, 159–161.

(11) Cole, P. A. Chemical probes for histone-modifying enzymes. *Nature Chem. Biol.* **2008**, *4*, 590–597.

(12) Frye, S. V.; Heightman, T.; Jin, J. Targeting Methyl Lysine. *Annu. Rep. Med. Chem.* **2010**, *45*, 329–343.

(13) Yost, J. M.; Korboukh, I.; Liu, F.; Gao, C.; Jin, J. Targets in Epigenetics: Inhibiting the Methyl Writers of the Histone Code. *Curr. Chem. Genomics* **2011**in press.

(14) Tachibana, M.; Sugimoto, K.; Nozaki, M.; Ueda, J.; Ohta, T.; Ohki, M.; Fukuda, M.; Takeda, N.; Niida, H.; Kato, H.; Shinkai, Y. G9a histone methyltransferase plays a dominant role in euchromatic histone H3 lysine 9 methylation and is essential for early embryogenesis. *Genes Dev.* **2002**, *16*, 1779–1791.

(15) Trojer, P.; Zhang, J.; Yonezawa, M.; Schmidt, A.; Zheng, H.; Jenuwein, T.; Reinberg, D. Dynamic Histone H1 Isotype 4 Methylation and Demethylation by Histone Lysine Methyltransferase G9a/KMT1C and the Jumonji Domain-Containing JMJD2/KDM4 Proteins. *J. Biol. Chem.* **2009**, *284*, 8395–8405.

(16) Sampath, S. C.; Marazzi, I.; Yap, K. L.; Krutchinsky, A. N.; Mecklenbrauker, I.; Viale, A.; Rudensky, E.; Zhou, M. M.; Chait, B. T.; Tarakhovsky, A. Methylation of a histone mimic within the histone methyltransferase G9a regulates protein complex assembly. *Mol. Cell* **2007**, *27*, 596–608.

(17) Huang, J.; Dorsey, J.; Chuikov, S.; Zhang, X.; Jenuwein, T.; Reinberg, D.; Berger, S. L. G9A and GLP methylate lysine 373 in the tumor suppressor p53. *J. Biol. Chem.* **2010**, *285*, 9636–9641.

(18) Kondo, Y.; Shen, L.; Ahmed, S.; Boumber, Y.; Sekido, Y.; Haddad, B. R.; Issa, J. P. Downregulation of histone H3 lysine 9 methyltransferase G9a induces centrosome disruption and chromosome instability in cancer cells. *PLoS One* **2008**, *3*, e2037.

(19) Kondo, Y.; Shen, L.; Suzuki, S.; Kurokawa, T.; Masuko, K.; Tanaka, Y.; Kato, H.; Mizuno, Y.; Yokoe, M.; Sugauchi, F.; Hirashima, N.; Orito, E.; Osada, H.; Ueda, R.; Guo, Y.; Chen, X.; Issa, J. P.; Sekido, Y. Alterations of DNA methylation and histone modifications contribute to gene silencing in hepatocellular carcinomas. *Hepatol. Res.* **2007**, *37*, 974–983.

(20) Watanabe, H.; Soejima, K.; Yasuda, H.; Kawada, I.; Nakachi, I.; Yoda, S.; Naoki, K.; Ishizaka, A. Deregulation of histone lysine methyltransferases contributes to oncogenic transformation of human bronchoepithelial cells. *Cancer Cell Int.* **2008**, *8*, 15.

(21) McGarvey, K. M.; Fahrner, J. A.; Greene, E.; Martens, J.; Jenuwein, T.; Baylin, S. B. Silenced tumor suppressor genes reactivated by DNA demethylation do not return to a fully euchromatic chromatin state. *Cancer Res.* **2006**, *66*, 3541–3549.

(22) Goyama, S.; Nitta, E.; Yoshino, T.; Kako, S.; Watanabe-Okochi, N.; Shimabe, M.; Imai, Y.; Takahashi, K.; Kurokawa, M. EVI-1 interacts with histone methyltransferases SUV39H1 and G9a for transcriptional repression and bone marrow immortalization. *Leukemia* **2010**, *24*, 81–88.

(23) Maze, I.; Covington, H. E., III; Dietz, D. M.; LaPlant, Q.; Renthal, W.; Russo, S. J.; Mechanic, M.; Mouzon, E.; Neve, R. L.; Haggarty, S. J.; Ren, Y.; Sampath, S. C.; Hurd, Y. L.; Greengard, P.; Tarakhovsky, A.; Schaefer, A.; Nestler, E. J. Essential role of the histone methyltransferase G9a in cocaine-induced plasticity. *Science* **2010**, *327*, 213–216.

(24) Schaefer, A.; Sampath, S. C.; Intrator, A.; Min, A.; Gertler, T. S.; Surmeier, D. J.; Tarakhovsky, A.; Greengard, P. Control of Cognition and Adaptive Behavior by the GLP/G9a Epigenetic Suppressor Complex. *Neuron* **2009**, *64*, 678–691.

(25) Imai, K.; Togami, H.; Okamoto, T. Involvement of histone H3 Lysine 9 (H3K9) methyl transferase G9a in the maintenance of HIV-1 latency and its reactivation by BIX01294. *J. Biol. Chem.* **2010**, *285*, 16538–16545.

(26) Link, P. A.; Gangisetty, O.; James, S. R.; Woloszynska-Read, A.; Tachibana, M.; Shinkai, Y.; Karpf, A. R. Distinct roles for histone methyltransferases G9a and GLP in cancer germ-line antigen gene regulation in human cancer cells and murine embryonic stem cells. *Mol. Cancer Res.* **2009**, *7*, 851–862.

(27) Tachibana, M.; Matsumura, Y.; Fukuda, M.; Kimura, H.; Shinkai, Y. G9a/GLP complexes independently mediate H3K9 and DNA methylation to silence transcription. *EMBO J.* **2008**, *27*, 2681–2690.

(28) Dong, K. B.; Maksakova, I. A.; Mohn, F.; Leung, D.; Appanah, R.; Lee, S.; Yang, H. W.; Lam, L. L.; Mager, D. L.; Schubeler, D.; Tachibana, M.; Shinkai, Y.; Lorincz, M. C. DNA methylation in ES cells requires the lysine methyltransferase G9a but not its catalytic activity. *EMBO J.* **2008**, *27*, 2691–2701.

(29) Kubicek, S.; O'Sullivan, R. J.; August, E. M.; Hickey, E. R.; Zhang, Q.; Teodoro, M. L.; Rea, S.; Mechtler, K.; Kowalski, J. A.; Homon, C. A.; Kelly, T. A.; Jenuwein, T. Reversal of H3K9me2 by a small-molecule inhibitor for the G9a histone methyltransferase. *Mol. Cell* **2007**, *25*, 473–481.

(30) Chang, Y.; Zhang, X.; Horton, J. R.; Upadhyay, A. K.; Spannhoff, A.; Liu, J.; Snyder, J. P.; Bedford, M. T.; Cheng, X. Structural basis for G9a-like protein lysine methyltransferase inhibition by BIX-01294. *Nature Struct. Mol. Biol.* **2009**, *16*, 312–317.

(31) Liu, F.; Chen, X.; Allali-Hassani, A.; Quinn, A. M.; Wasney, G. A.; Dong, A.; Barsyte, D.; Kozieradzki, I.; Senisterra, G.; Chau, I.; Siarheyeva, A.; Kireev, D. B.; Jadhav, A.; Herold, J. M.; Frye, S. V.; Arrowsmith, C. H.; Brown, P. J.; Simeonov, A.; Vedadi, M.; Jin, J. Discovery of a 2,4-diamino-7-aminoalkoxyquinazoline as a potent and selective inhibitor of histone lysine methyltransferase G9a. *J. Med. Chem.* **2009**, *52*, 7950–7953.

(32) Liu, F.; Chen, X.; Allali-Hassani, A.; Quinn, A. M.; Wigle, T. J.; Wasney, G. A.; Dong, A.; Senisterra, G.; Chau, I.; Siarheyeva, A.; Norris, J. L.; Kireev, D. B.; Jadhav, A.; Herold, J. M.; Janzen, W. P.; Arrowsmith, C. H.; Frye, S. V.; Brown, P. J.; Simeonov, A.; Vedadi, M.; Jin, J. Protein Lysine Methyltransferase G9a Inhibitors: Design, Synthesis, and Structure−Activity Relationships of 2,4-Diamino-7-aminoalkoxy-quinazolines. *J. Med. Chem.* **2010**, *53*, 5844–5857.

(33) Chang, Y.; Ganesh, T.; Horton, J. R.; Spannhoff, A.; Liu, J.; Sun, A.; Zhang, X.; Bedford, M. T.; Shinkai, Y.; Snyder, J. P.; Cheng, X. Adding a lysine mimic in the design of potent inhibitors of histone lysine methyltransferases. *J. Mol. Biol.* **2010**, *400*, 1–7.

(34) Vedadi, M.; Barsyte-Lovejoy, D.; Liu, F.; Rival-Gervier, S.; Allali-Hassani, A.; Labrie, V.; Wigle, T. J.; DiMaggio, P. A.; Wasney, G. A.; Siarheyeva, A.; Dong, A.; Tempel, W.; Wang, S.-C.; Chen, X.; Chau, I.; Mangano, T.; Huang, X.-P.; Simpson, C. D.; Pattenden, S. G.; Norris, J. L.; Kireev, D. B.; Tripathy, A.; Edwards, A.; Roth, B. L.; Janzen, W. P.; Garcia, B. A.; Petronis, A.; Ellis, J.; Brown, P. J.; Frye, S. V.; Arrowsmith, C. H.; Jin, J. A Chemical Probe Selectively Inhibits G9a and GLP Methyltransferase Activity in Cells. *Nature Chem. Biol.* **2011**, *7*, 566–574.

(35) Tachibana, M.; Ueda, J.; Fukuda, M.; Takeda, N.; Ohta, T.; Iwanari, H.; Sakihama, T.; Kodama, T.; Hamakubo, T.; Shinkai, Y. Histone methyltransferases G9a and GLP form heteromeric complexes and are both crucial for methylation of euchromatin at H3-K9. *Genes Dev.* **2005**, *19*, 815–826.

(36) Gottlieb, H. E.; Kotlyar, V.; Nudelman, A. NMR Chemical Shifts of Common Laboratory Solvents as Trace Impurities. *J. Org. Chem.* **1997**, *62*, 7512–7515.

(37) Nazare, M.; Will, D. W.; Matter, H.; Schreuder, H.; Ritter, K.; Urmann, M.; Essrich, M.; Bauer, A.; Wagner, M.; Czech, J.; Lorenz, M.; Laux, V.; Wehner, V. Probing the subpockets of factor Xa reveals two binding modes for inhibitors based on a 2-carboxyindole scaffold: a study combining structure−activity relationship and X-ray crystallography. *J. Med. Chem.* **2005**, *48*, 4511–4525.

(38) Collazo, E.; Couture, J. F.; Bulfer, S.; Trievel, R. C. A coupled fluorescent assay for histone methyltransferases. *Anal. Biochem.* **2005**, *342*, 86–92.